Available online at www.sciencedirect.com
ScienceDirect
Procedia Engineering 166 (2016) 91 – 98
Procedia Engineering
www.elsevier.com/locate/procedia

2nd International Symposium on Submerged Floating Tunnels and Underwater Tunnel Structures

A numerical study on responses of submerged floating structures undergoing vortex-induced vibration and seismic excitation

Ling Kang[a,b], Fei Ge[a,*], Youshi Hong[a,b,†]

[a]LNM, Institute of Mechanics, Chinese Academy of Sciences, Beijing 100190, China
[b]University of Chinese Academy of Sciences, Beijing, China

Abstract

The dynamic responses of submerged floating structures undergoing vortex-induced vibration and seismic excitation were numerically investigated. The tube and tethers of submerged floating structures were assumed as an Euler-Bernoulli beam and the hinged supports of the tube, respectively. The wakes behind the tube were regarded as distributed oscillators. With the consideration of the fluid-structure interaction, the prediction model of the responses was established. Numerical results show that the tube responses of the submerged floating structures subjected to the vortex induced forces and seismic excitation have the feature of nonlinearity. Superposition method is not suitable for the solution of such responses. As the tether spacing reduces, the maximum displacement of the tube, the constraint forces and the constraint moments of all the supports of the tube reduce. In the same variation interval of the tether spacing, the maximum displacements reduce most its values. The tube vibration of the submerged floating structure presents more periodicity when the tether spacing reduces.

Peer-review under responsibility of the organizing committee of SUFTUS-2016

Keywords: Fluid-structure interaction; nonlinearity; tether spacing

1. Introduction

Submerged floating structure is an interesting topic of recent investigations. As an innovative water-crossing structure, submerged floating structure possesses the advantages in the aspects of economy, environmental

* Corresponding author. Tel.: +86-10-82543968; fax: +86-10-62561284.
E-mail address: gefei@imech.ac.cn
* Corresponding author. Tel.: +86-10-82543966; fax: +86-10-62561284.
E-mail address: hongys@imech.ac.cn

Peer-review under responsibility of the organizing committee of SUFTUS-2016
doi:10.1016/j.proeng.2016.11.569

friendliness and adaptability to complicated situations (e.g. bad weather, dynamic loads, etc.) [1]. Such complicated situations make the response analysis of submerged floating structures challenging. Therefore, efforts have been devoted to the response analysis [2], especially the dynamic response analysis under different dynamic loads (e.g. moving loads [3], waves [4,5], shedding vortices [6] and seismic excitation [7]). However, the responses of submerged floating structures subjected to combined dynamic loads are less understood.

In this paper, a numerical method was carried out to study the response properties of submerged floating tubes, on which shedding vortices and seismic excitation were imposed. Further, the effects of tether spacing on such dynamic responses were investigated. Results show that the tube responses have the feature of nonlinearity. When the tether spacing reduces, the maximum displacement of the tube, the constraint forces and the constraint moments of all the supports of the tube reduce.

2. Mathematical Model and solution methods

Here, we use an Euler-Bernoulli beam to model the tube of a submerged floating structure. For simplicity, the mooring tethers of the submerged floating structure are regarded as hinged supports of the tube. All the hinged supports are equally spaced. As shown in Fig. 1, shedding vortices behind the tube (wakes) are produced by a uniform flow with the flow velocity of *U*. Seismic excitation is assumed to act on supports and be synchronous at each support with the acceleration of ground motion $\ddot{u}_{\mathrm{g}}$.

Coordinate *x* is the axial direction of the tube, while coordinates *y* and *z* are the directions perpendicular to *U* (cross-flow) and parallel with *U* (in-line), respectively. Distributed van der Pol equations are employed to describe the wake dynamics in both cross-flow and in-line directions [8]. With the consideration of fluid-structure interaction, the equations for the dimensionless mathematical model are as follows.

$$\frac{\partial^2 y}{\partial \tau^2}+\frac{\gamma}{\mu}\frac{\partial y}{\partial \tau}+b^2\frac{\partial^4 y}{\partial \tilde{x}^4}=M_{\mathrm{L}}q_{\mathrm{L}}-\ddot{y}_{\mathrm{g}} \tag{1}$$

$$\frac{\partial^2 q_{\mathrm{L}}}{\partial \tau^2}+\xi_{\mathrm{L}}\left(q_{\mathrm{L}}^2-1\right)\frac{\partial q_{\mathrm{L}}}{\partial \tau}+q_{\mathrm{L}}=A_{\mathrm{L}}\frac{\partial^2 y}{\partial \tau^2} \tag{2}$$

$$\frac{\partial^2 z}{\partial \tau^2}+\frac{\gamma}{\mu}\frac{\partial z}{\partial \tau}+b^2\frac{\partial^4 z}{\partial \tilde{x}^4}=M_{\mathrm{D}}q_{\mathrm{D}}-\ddot{z}_{\mathrm{g}} \tag{3}$$

$$\frac{\partial^2 q_{\mathrm{D}}}{\partial \tau^2}+2\xi_{\mathrm{D}}\left(q_{\mathrm{D}}^2-1\right)\frac{\partial q_{\mathrm{D}}}{\partial \tau}+4q_{\mathrm{D}}=A_{\mathrm{D}}\frac{\partial^2 z}{\partial \tau^2} \tag{4}$$

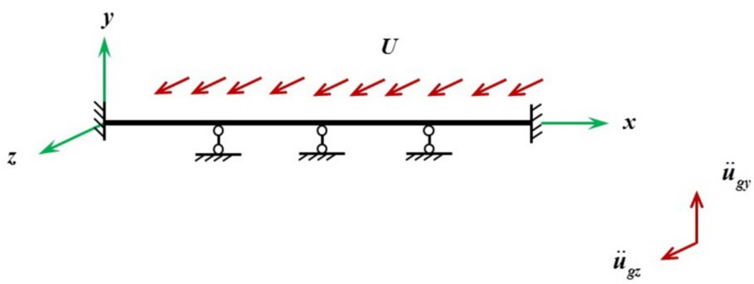

Fig. 1. Simplification of a submerged floating structure.

where $y = u_y/d$, $z = u_z/d$, u_y and u_z are dynamic displacements of the tube in cross-flow direction and in-line direction, respectively, d is the outer diameter of the tube., $\tau=\omega_s t$ and $\tilde{x}=x/L$. The time t and the coordinate x are normalized by the vortex shedding frequency ω_s and the length of the tube L, respectively.

Moreover, $\ddot{y}_g=\ddot{u}_{gy}/d\omega_s^2$ and $\ddot{z}_g=\ddot{u}_{gz}/d\omega_s^2$. $\ddot{u}_{gy}$ and $\ddot{u}_{gz}$ are the accelerations of the ground motion in cross-flow direction and in-line direction, respectively. q_L and q_D represent the reduced lift coefficient and the reduced drag coefficient induced by vortices, respectively.

γ is a stall parameter defined in [9]. μ is the mass ratio, expressed as $\mu=m/\rho_w d^2$. $m=m_s+m_a$, where m_s is the mass per unit length of the tube and m_a the added mass per unit length. ρ_w is the density of the water. ξ_L , ξ_D , A_L , A_D show the properties of the distributed van der Pol oscillators. The dimensionless parameters, b^2 , M_L and M_D , have the following form:

$$b^2 = \frac{EI}{mL^4\omega_s^2},\ M_L = \frac{C_{L0}}{2}\frac{1}{8\pi^2 St^2\mu},\ M_D = \frac{C_{D0}}{2}\frac{1}{8\pi^2 St^2\mu} \tag{5}$$

where EI indicates the bending stiffness of the tube. C_{L0} and C_{D0} are the lift coefficient and the drag coefficient induced by vortices behind a fixed cylinder, respectively. St represents the Strouhal number.

The boundary conditions of the submerged floating tube are written as Eqs. (6) to (9) in a dimensionless form.

- Fixed ends

$$y(0,\tau) = 0, y(1,\tau) = 0, \frac{\partial y}{\partial \tilde{x}}(0,\tau) = 0, \frac{\partial y}{\partial \tilde{x}}(1,\tau) = 0 \tag{6}$$

$$z(0,\tau) = 0, z(1,\tau) = 0, \frac{\partial z}{\partial \tilde{x}}(0,\tau) = 0, \frac{\partial z}{\partial \tilde{x}}(1,\tau) = 0 \tag{7}$$

- Hinged supports

$$y_i(\tilde{x}_i,\tau) = 0, \tilde{M}_{xyi}(\tilde{x}_i,\tau) = 0 \tag{8}$$

$$z_i(\tilde{x}_i,\tau) = 0, \tilde{M}_{xzi}(\tilde{x}_i,\tau) = 0 \tag{9}$$

where $\tilde{x}_i$ is the dimensionless coordinate of the i-th hinged support. y_i and z_i are the dimensionless displacements of the tube at the i-th hinged support in cross-flow direction and in-line direction, respectively. $\tilde{M}_{xyi}=M_{xyi}/mdL^2\omega_s^2$ and $\tilde{M}_{xzi}=M_{xzi}/mdL^2\omega_s^2$, where M_{xyi} and M_{xzi} are the constraint moments of the tube at the i-th hinged support in the xy plane and xz plane, respectively.

Eqs. (1) to (4) were solved by the finite element method (FEM) [10] and the fourth order Runge-Kutta method (RK-4) [11]. First, we perform the FEM to discretize Eqs. (1) to (4) in space. Then, RK-4 was introduced to obtain the discrete time series of the nodal tube displacements, the nodal tube velocities, the nodal tube accelerations and the nodal coefficients of the reduced lift and drag forces.

The constraint forces and moments at the fixed ends and the constraint forces at the hinged supports were calculated with those RK-4 time series through the FEM assembled equations of motion of the tube. Note that the FEM assembled equations of motion should have the feature of singularity.

3. Parameter values

As shown in Table 1, the design parameters of the submerged floating tunnel (SFT) prototype in Qiandao Lake of China [12] were employed to calculate the values of the dimensionless parameters in Eqs. (1) and (3). Note that the flow velocity in Qiandao Lake was adjusted so that we can excite the vortex-induced vibration of the tube. The parameters related to the van der Pol oscillators in Eqs. (2) and (4) have the values of $\xi_L=\xi_D=0.3$ and $A_L=A_D=12$ [9]. The EI Centro wave was chosen to simulate the ground motion. The vertical acceleration time history of this seismic wave was imposed on the supports in cross-flow direction, while the 180^o acceleration time history excited the vibration of the tube in in-line direction.

Table 1. Design parameters of the SFT prototype in Qiandao Lake

Design parameter	Symbol	Unit	Value
Length	L	m	100
Outer diameter	d	m	4.39
Inner diameter	D_I	m	3.55
Self-weight per unit length	W	kN/m	115
Equivalent elastic modulus	E	GPa	140
Water density	ρ_W	kg/m^3	1000
Added mass coefficient	C_a	-	1.0
Strouhal number	S_t	-	0.17
Lift coefficient of fixed cylinder	C_{L0}	-	0.3
Drag coefficient of fixed cylinder	C_{D0}	-	0.2
Flow velocity	U	m/s	8.0

4. Results

Once we get the discrete time series of the responses, we can further calculate the root mean squares (RMSs) and frequency spectrums of those time series. Figs. 2 and 3 illustrate the RMS results in the cross-flow direction and in-line direction, respectively. The maximum RMSs of the tube displacements are the maxima in time and space. All the RMSs in Figs. 2 and 3 were shown in a dimensionless form. The RMSs of the constraint forces at the fixed ends and hinged supports were normalized by the parameter $mdL\omega_s^2$, while those of the constraint moments at the fixed ends were divided by $mdL^2\omega_s^2$. The tether spacing in Figs. 2 and 3 was normalized by the length of the tube, L.

Eqs. (1) and (3) indicate that the submerged floating tube here is a linear system. Whether is it applicable for the V-S response (which is short for the response of the tube undergoing vortex-induced vibration (VIV) and seismic excitation) to be the superposition of the VIV response and the seismic response? To study this issue, we not only obtained the V-S responses, but also calculated the VIV responses, the seismic responses and their summation, called superposition responses. They are shown in Figs. 2 and 3.

The results show that the V-S responses are not equal to the superposition responses. The values of the V-S responses are smaller than those of the superposition responses. Their relative errors (Tables 2 and 3) are at least 11.6% and 31.1% in the cross-flow direction and in-line direction, respectively. Such relative errors increase as the tether spacing increases. However, they keep constant when the tether spacing is smaller than the critical value of $L/4$. This indicates that the calculated error between the V-S response and superposition response is large. For accuracy, it is better not to compute the V-S response by superposition method. The responses of the tube subjected to vortex-induced vibration and seismic excitation have the feature of nonlinearity, although the tube itself is linear.

It is presumed that the coupling of the tube motion and the wake oscillator makes the V-S responses nonlinear. In fact, the ground motion influences the fluid field indirectly through the tube motion when seismic excitation and shedding vortices are simultaneously imposed on the tube, since the tube motion includes the part resulted from the ground motion. Such indirect effect of the ground motion on fluid field is not revealed in the superposition method.

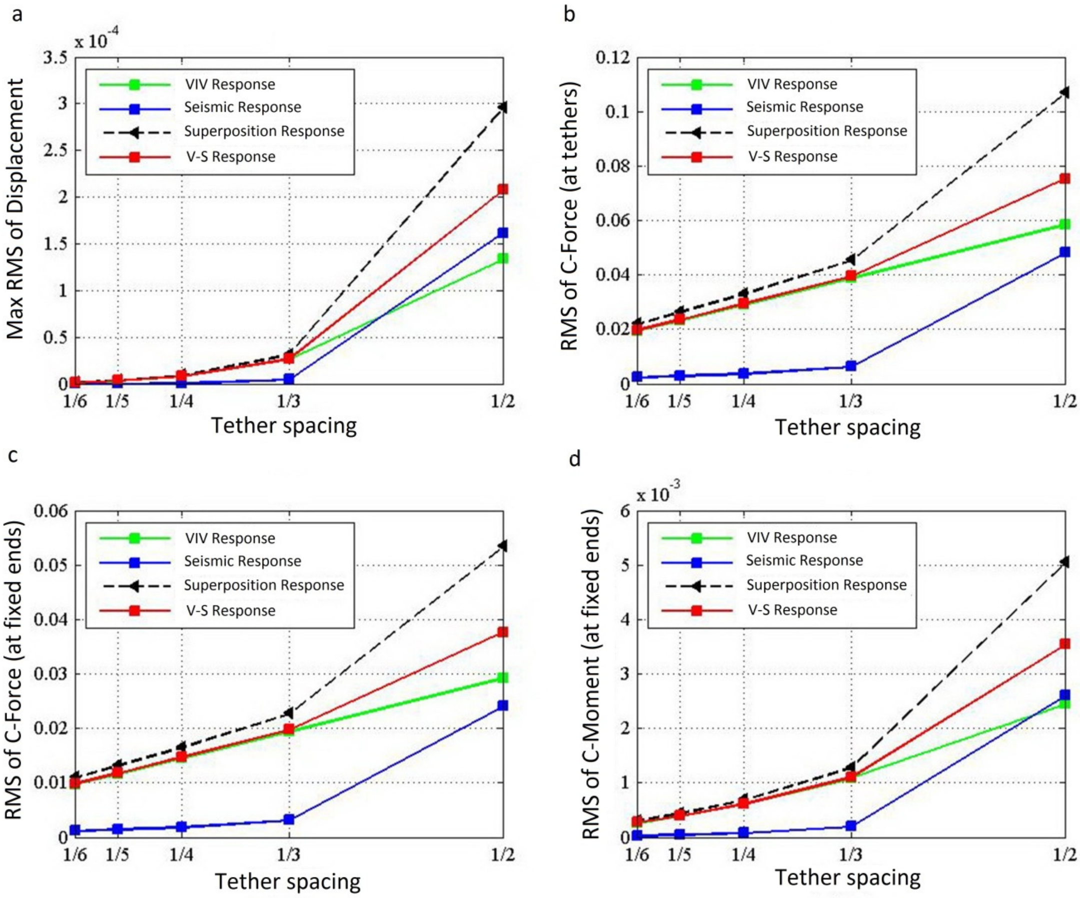

Fig. 2. RMS results (dimensionless) versus tether spacing (dimensionless) in cross-flow direction: (a) Maximum RMS of tube displacement; (b) RMS of constraint force at tethers (hinged supports); (c) RMS of constraint force at fixed ends; (d) RMS of constraint moment at fixed ends.

Table 2. Relative errors between V-S responses and superposition responses in cross-flow direction.

Response	Tether spacing (dimensionless)				
	1/6	1/5	1/4	1/3	1/2
Maximum displacement	11.6%	11.6%	11.9%	16.6%	42.2%
Constraint force (at tethers)	11.6%	11.6%	11.8%	14.6%	41.6%
Constraint force (at fixed ends)	11.6%	11.6%	11.8%	14.6%	41.6%
Constraint moment (at fixed ends)	11.6%	11.6%	11.9%	15.6%	42.6%

When the tether spacing reduces, the maximum RMSs of the tube displacements, of the constraint forces and of the constraint moments all reduce. Computing the average gradients of the V-S response curves in Figs. 2 and 3, we find that the RMSs of the tube displacements reduce most its values in the cross-flow and in-line directions. Then, the RMSs of the constraint moments at the fixed ends have an intermediate reduce. The RMSs of the constraint forces at the fixed ends and the tether locations (hinged supports) reduce at a minimum level. The average gradients are shown in Table 4.

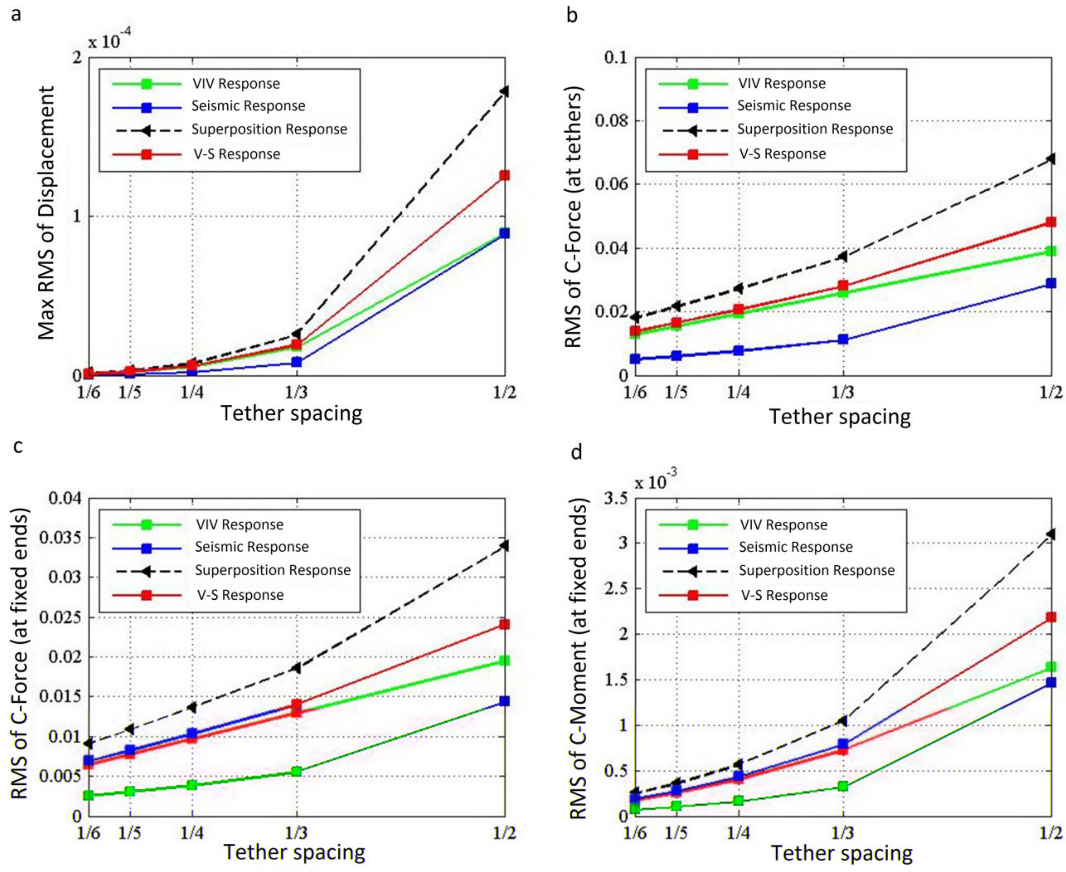

Fig. 3. RMS results (dimensionless) versus tether spacing (dimensionless) in in-line direction: (a) Maximum RMS of tube displacement; (b) RMS of constraint force at tethers (hinged supports); (c) RMS of constraint force at fixed ends; (d) RMS of constraint moment at fixed ends.

Table 3. Relative errors between V-S responses and superposition responses in in-line direction.

Response	Tether spacing (dimensionless)				
	1/6	1/5	1/4	1/3	1/2
Maximum displacement	31.1%	30.9%	31.0%	33.1%	42.1%
Constraint force (at tethers)	31.1%	31.0%	31.1%	32.3%	40.8%
Constraint force (at fixed ends)	31.1%	31.0%	31.1%	32.3%	40.8%
Constraint moment (at fixed ends)	31.1%	30.9%	31.1%	32.8%	42.0%

Fig. 4 presents the frequency spectrum of the tube undergoing vortex-induce vibration and seismic excitation. The left column shows the results in cross-flow direction, while the right column gives the results in in-line direction. The vibration frequencies of the tube include an isolated peak frequency and frequencies with the wideband feature when the tether spacing is $L/2$. As the tether spacing decreases, the frequencies with the wideband feature diminish. It indicates that such vibration of the tube presents more periodicity when the tether spacing is reduced.

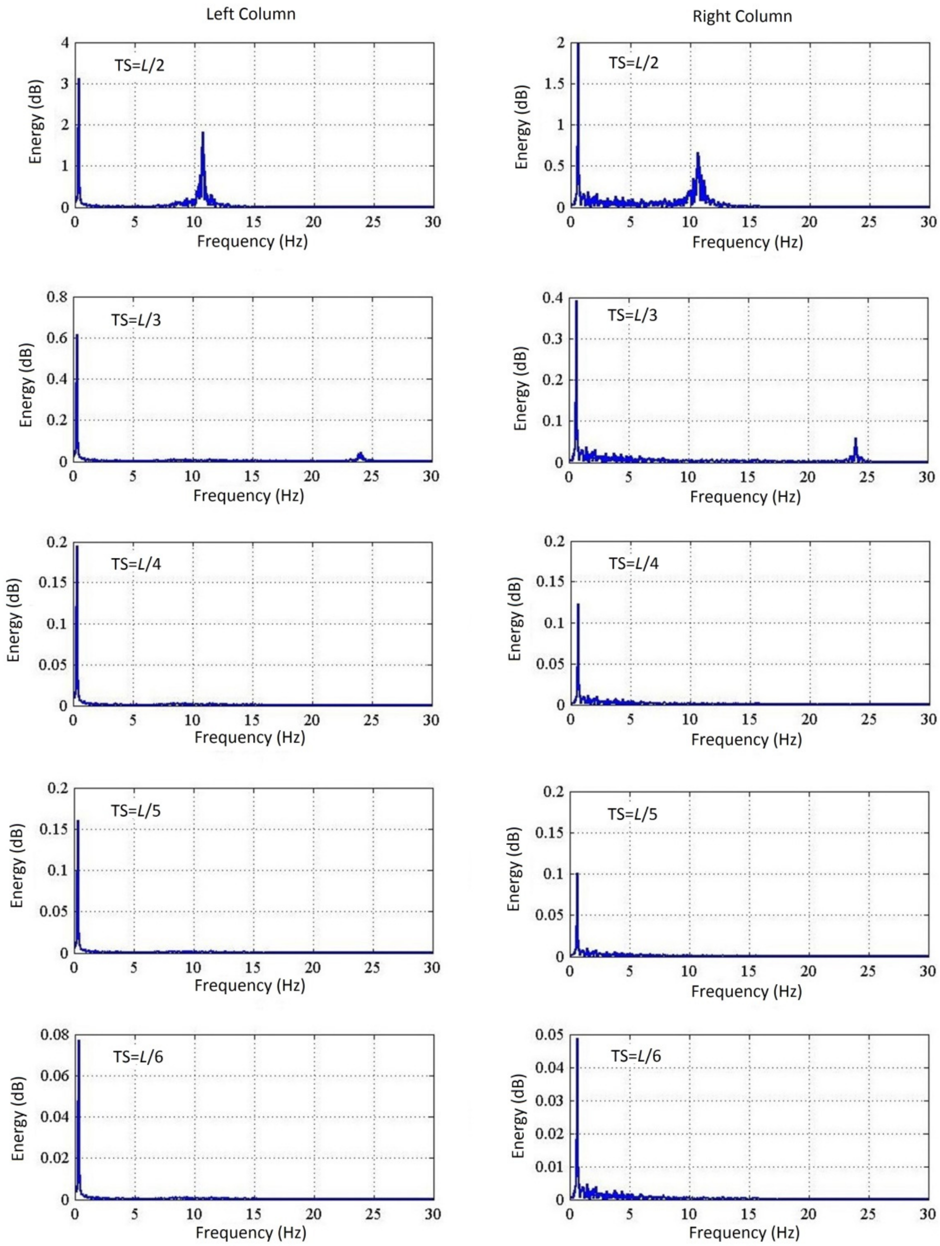

Fig. 4. The frequency spectrums of the tube. Left Column: in cross-flow direction; Right Column: in in-line direction. TS: tether spacing. *L* is the length of the tube.

Table 4. Average gradients of V-S response curves.

Direction	Max displacements	Constraint moments	Constraint forces
Cross-flow	0.992	0.922	0.739
In-line	0.991	0.912	0.713

5. Conclusions

The dynamic responses of submerged floating structures subjected to the vortex-induced vibration and seismic excitation were numerically studied. Conclusions are drawn as follows.

The tub responses of the submerged floating structure are nonlinear when the vortex-induced vibration and seismic excitation are simultaneously imposed on the tube. If the tether spacing reduces, the maximum RMS of the tube displacement, that of the constraint moment and that of the constraint force will reduce accordingly. The fastest decreasing response is the maximum displacement. The constraint moment has an intermediate reduction, while the decrement of the constraint force is the smallest. The vibration of the submerged floating tube presents more periodicity as the tether spacing is reduced.

Acknowledgements

This work was supported by the Construction Technology Program of Ministry of Transport (Grant No. 2013 318 740050).

References

[1] D. Ahrens, Submerged Floating Tunnels-A concept whose time has arrived, Tunn. Undergr. Sp. Tech. 12(2) (1997) 317-336.

[2] S. Zhang, L. Wang, Y.S. Hong, Structural analysis and safety assessment of submerged floating tunnel prototype in Qiandao Lake (China). Procedia Eng. 4 (2010) 179-187.

[3] S. Tariverdilo, J. Mirzapour, M. Shahmardani, R. Shabani, C. Gheyretmand, Vibration of submerged floating tunnels due to moving loads, Appl. Math. Model. 35(11) (2011) 5413-5425.

[4] F. Ge, W. Lu, X. D. Wu, Y.S. Hong, Fluid-structure interaction of submerged floating tunnel in wave field. Procedia Eng. 4 (2010) 263-271.

[5] W. Lu, F. Ge, L. Wang, X. D. Wu, Y.S. Hong, On the slack phenomena and snap force in tethers of submerged floating tunnels under wave conditions, Mar. Struct. 24(4) (2011) 358-376.

[6] X.D. Wu, F. Ge, Y.S. Hong, An Experimental investigation of dual-resonant and non-resonant responses for vortex-induced vibration of a long slender cylinder, Sci. China Phys. Mech. 57(2) (2014) 321-329.

[7] L. Martinelli, G. Barbella, A. Feriani, A numerical procedure for simulating the multi-support seismic response of submerged floating tunnels anchored by cables, Eng. Struct. 33(10) (2011) 2850-2860.

[8] F. Ge , X. Long, L. Wang, Y.S. Hong, Flow-induced vibrations of long circular cylinders modeled by coupled nonlinear oscillators, Sci. China Phys. Mech. 52(7) (2009) 1086-1093.

[9] M.L. Facchinetti, E. de Langre, F. Biolley, Coupling of structure and wake oscillators in vortex-induced vibrations, J. Fluid Struct. 19 (2004) 123-140.

[10] J.L. Humar, Dynamics of structures, third ed., CRC Press, 2012.

[11] J.C. Butcher, Numerical Methods for Ordinary Differential Equations, second ed., John Wiley & Sons Ltd, England, 2008.

[12] F.M. Mazzolani, R. Landolfo, B. Faggiano, M. Esposto, F. Perotti, G. Barbella, Structural analyses of the Submerged Floating Tunnel prototype in Qiandao Lake (PR of China), Adv. Struct. Eng. 11(4) (2008) 439-454.